VIP RNA Recognition Very Important Paper

DOI: 10.1002/anie.201305079

Binding of a Designed Anti-Cancer Drug to the Central Cavity of an RNA Three-Way Junction**

Siriporn Phongtongpasuk, Susann Paulus, Joachim Schnabl, Roland K. O. Sigel, Bernhard Spingler,* Michael J. Hannon,* and Eva Freisinger**

Dedicated to Professor Jan Reedijk on the occasion of his 70th birthday

Nucleic acids are exciting biomolecular targets because they offer the potential to regulate information transfer at the beginning, before the genetic code is translated into proteins. Metal complexes that bind to DNA have been of particular interest, with the cationic charge that metals impart being particularly attractive for recognition of these polyanions.[1] Examples include complexes that coordinate to the bases,[2] intercalate,[3] or bind to the phosphate backbone[4] of regular duplex DNA or, more recently, that recognize less common DNA structures such as bulges,[5] quadruplexes,[6] or junctions.[7] Such complexes have been explored as therapeutic drugs,[2] fluorescent imaging agents,[8] footprinting agents,[9] and for nanotechnology applications.[10]

RNA binding by metal complexes is much less well understood.[11] Yet, RNA is an emerging biomedical target because its high structural diversity makes it highly suitable for supramolecular recognition. For example, a Diels–Alderase ribozyme was developed by in vitro selection[12] and riboswitches have evolved naturally that are key to bacterial gene regulation. Both types of functional RNAs depend on specific ligand binding, for example, to a three-way junction (3WJ)-type cage as in the Diels–Alderase and the purine riboswitch,[13] with subsequent structural rearrangement.

[*] Dr. S. Phongtongpasuk,[+] S. Paulus,[+] J. Schnabl,[+] Prof. Dr. R. K. O. Sigel, Priv.-Doz. Dr. B. Spingler, Prof. Dr. E. Freisinger
Institut für Anorganische Chemie, Universität Zürich
Winterthurerstrasse 190, 8057 Zürich (Switzerland)
E-mail: roland.sigel@aci.uzh.ch
spingler@aci.uzh.ch
freisinger@aci.uzh.ch
Homepage: http://www.chem.uzh.ch
Dr. S. Phongtongpasuk,[+] Prof. Dr. M. J. Hannon
School of Chemistry, University of Birmingham
Edgbaston, Birmingham B152TT (UK)
E-mail: m.j.hannon@bham.ac.uk
[+] These authors contributed equally to this work.

[**] Financial support within the COST Actions D39 and CM1105, from the Swiss State Secretariat for Education and Research (E.F. and R.K.O.S.), the Swiss National Science Foundation (E.F. and R.K.O.S.), the University of Birmingham, the University of Zurich, and the Strategic Scholarships fellowships Frontier Research Networks from the Commission of Higher Education, Government of Thailand (S.P.) are gratefully acknowledged. R.K.O.S. is a recipient of an ERC Starting Grant 2010. We also thank Dr. Meitian Wan and Dr. Vincent Olieric for excellent support at the SLS synchrotron.

Supporting information for this article is available on the WWW under http://dx.doi.org/10.1002/anie.201305079.

Hannon, Coll, and co-workers described the binding of a nano-sized dimetallic metal complex (a metallo-supramolecular cylinder) to the central cavity of a DNA 3WJ.[7a] Given that junctions are common in RNA structures, their recognition seemed an attractive initial step towards RNA structural recognition agents. Herein, we report the ability of a di-iron(II) supramolecular cylinder to recognize an RNA 3WJ and use X-ray crystallography to characterize the binding mode. While there are some crystal structures of RNAs with simple hexaqua or hexammine cations,[14] to the best of our knowledge this is the first crystallographic study of a designed metal complex bound to RNA.

We first crystallized the di-iron(II) supramolecular cylinder with a palindromic RNA hexanucleotide sequence (Figure 1 A), which was selected to allow a direct comparison with the structure of the analogous DNA in complex with the cylinder.[7a,c,d] Crystals diffracting to 1.91 Å were obtained under similar crystallization conditions and contain exclusively the *M* enantiomer of the cylinder. The structure reveals an RNA 3WJ with the cylinder sitting at the heart of the junction (Figure 1 B). Additional cylinder molecules reside at the GC termini of the duplex RNA arms that radiate from the junction, with the bases making π-stacking interactions with the cylinder phenylene rings forming what is in effect an additional non-covalent pseudo-junction.

While the overall structure obtained is highly similar to the one of the DNA 3WJ, distinct differences exist in the mode of recognition of the cylinder by the RNA 3WJ. These variations mainly originate from the specific conformation of the DNA versus the RNA oligonucleotide. Whereas the double-stranded parts of the DNA in the 3WJ adopt a B-form, the RNA shows its usual A-form. Overall, the DNA 3WJ resembles a truncated cone (Figure 1 C) with a narrower top being formed by the 3′ ends (Figure 2 A), while the 5′ ends point away from the central opening. The top and bottom openings of the RNA 3WJ are more similar in size (Figure 1 B) with the 3′ and 5′ ends bent away from the central opening, effectively side-stepping any interaction with the cylinder. Accordingly, the narrowest part of the RNA junction is formed by the central adenine and uracil bases. In the DNA 3WJ, two main interactions with the cylinder are described: 1) the bases at the junction form a π-stacking interaction with the central phenylene rings of the cylinder (Figure 2 B), and 2) the terminal pyridine rings of the cylinder engage in van der Waals interactions with the C5′ sugar moieties. The opening at the top of the cone is sufficiently narrow that the cylinder does not penetrate it (Figure 2 A). It

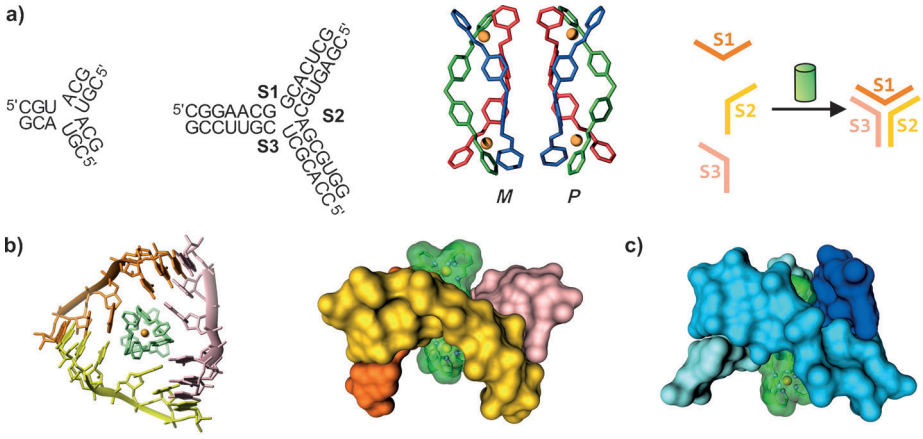

Figure 1. Formation of an RNA 3WJ stabilized by a cylindrical di-iron(II) complex, $[Fe_2L_3]^{4+}$ ($L = C_{25}H_{20}N_4$). a) Palindromic RNA sequence used for crystallization (left) next to the three RNA strands S1, S2, and S3 as used in the gel studies. The *M* and *P* enantiomers of the cylinder and the formation of the 3WJ stabilized by a cylinder molecule are shown on the right. b) The crystal structure of the RNA 3WJ complexed with the cylinder as seen from the top (left) and a surface representation from the side (right). c) Side view of the corresponding DNA 3WJ/cylinder complex as a surface representation (PDB: 2ET0). Panels (b) and (c) were prepared with MOLMOL and DS Visualizer 3.5.[15]

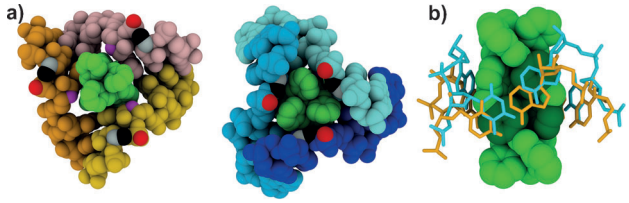

Figure 2. Comparison of the morphologies of the RNA/DNA 3WJ-cylinder complexes. a) Space-filling models of the RNA (left) and DNA (right) 3WJs with the cylinder (green) seen from the top. Cytidine 5 forms the top edge of the 3WJ, which is much narrower in the DNA (C5-C4′, grey atoms; C5-C5′, black; C5-O1P, red; RNA/DNA = 8.0/5.9 Å, 8.5/5.3 Å, and 11.6/5.9 Å, respectively, from the central cylinder axis). b) Stacking interactions between the AU (gold) and AT (cyan) base pairs with the two central B and C rings of the cylinder (green).

is unclear whether the narrow opening originates from the rigidity of the 3WJ structure or is caused by attractive interactions with the cylinder. This question will be of importance for the discussion below. The central π-stacking interactions with the cylinder can also be observed in the RNA 3WJ (Figure 2B). Here the uracil base also interacts with one phenylene, while the cylinder is shifted such that each adenine base now stacks with two central phenylenes of one ligand and a C1′H-π interaction is formed. Superimposing both structures based on the central AT and AU base pairs reveals a shift of the cylinder by 2.0 Å towards the 3′-end in the RNA structure. Given that the π-stacking interaction between the RNA bases and the phenylene rings of the cylinder constitutes the only interactions observed, and considering that the position of the cylinder within the junction is not constricted by the narrowness of the 3′-end as in the DNA structure (Figure 2B), the cylinder should be allowed to move freely within the RNA junction to maximize the stabilization from the π-stacking interactions with the bases of the junction. Consequently, the position of the cylinder within the DNA 3WJ, which does not seem to be free to move and optimize the stacking interactions, should result in a lower contribution of the stacking interaction to the stability of the structure. The overall stabilization in the DNA versus the RNA structure is also dependent on whether the 3′ ends in the DNA structure merely sterically restrict the optimal positioning of the cylinder within the junction or provide additional stabilization through van der Waals interactions. The structure of the cylinder is virtually the same in both DNA and RNA 3WJs, that is, it is not influenced by the different stacking interactions.[15]

To complement our studies we were curious to see RNA 3WJ formation, and the influence of the cylinder, in solution (Supporting Information, Figures S1–S5). We chose three RNA sequences that potentially form a 3WJ analogous to a known DNA 3WJ (Figure 1A).[7c] Cylinder-promoted formation of the 3WJ was followed by native gel electrophoresis, in which the S1 RNA strand was 5′ end labeled with ^{32}P-phosphate. 200 nM of each RNA strand was used in the presence of 100 mM NaCl at 4 °C (Figure 3A). In the absence of Mg^{2+} ions or the cylinder, distinct self-assembly of the three strands into either an open dimer or a 3WJ was observed. Whereas additional $MgCl_2$ (10 mM) had virtually no effect, excess cylinder clearly stabilized the 3WJ and reduced the amount of dimer (78% 3WJ, 14% dimer, 8% single strand; distributions of the three states under all conditions tested are summarized in Figure S1). The strong stabilization of the 3WJ by the cylinder was verified using a bulkier cylinder $[Fe_2(L\text{-}CF_3)_3]^{4+}$ with the same charge but having two central trifluoromethyl groups on each ligand that will not fit into a 3WJ. Indeed, no additional 3WJ formation was induced (Figure 3; Figures S1,S2). This stabilizing effect goes beyond the pure electrostatic interaction with duplex RNA, because the stabilizing effect of 20 μM cylinder is clearly larger than that of 10 mM Mg^{2+} (Figure 3), which is in agreement with the extensive stacking interactions observed in the crystal structure. Interestingly, while the *M* enantiomer shows a higher affinity than *P* towards DNA,[7c] no difference between the *M* and *P* cylinders could be detected for RNA 3WJ formation under any conditions tested, within the error limits (Figure 3C; Figures S1,S3).

At 4 °C, the open RNA dimers are relatively stable. Raising the temperature to 25 °C lead to melting of the two strands at both low and high RNA concentration (Figure 3B; Figure S2B). Even in the presence of a tenfold excess of a racemic mixture of the cylinders no open dimer, but instead 80% 3WJ, was present in solution. Again, the bulky cylinder did not additionally promote 3WJ formation (Figure 3B).

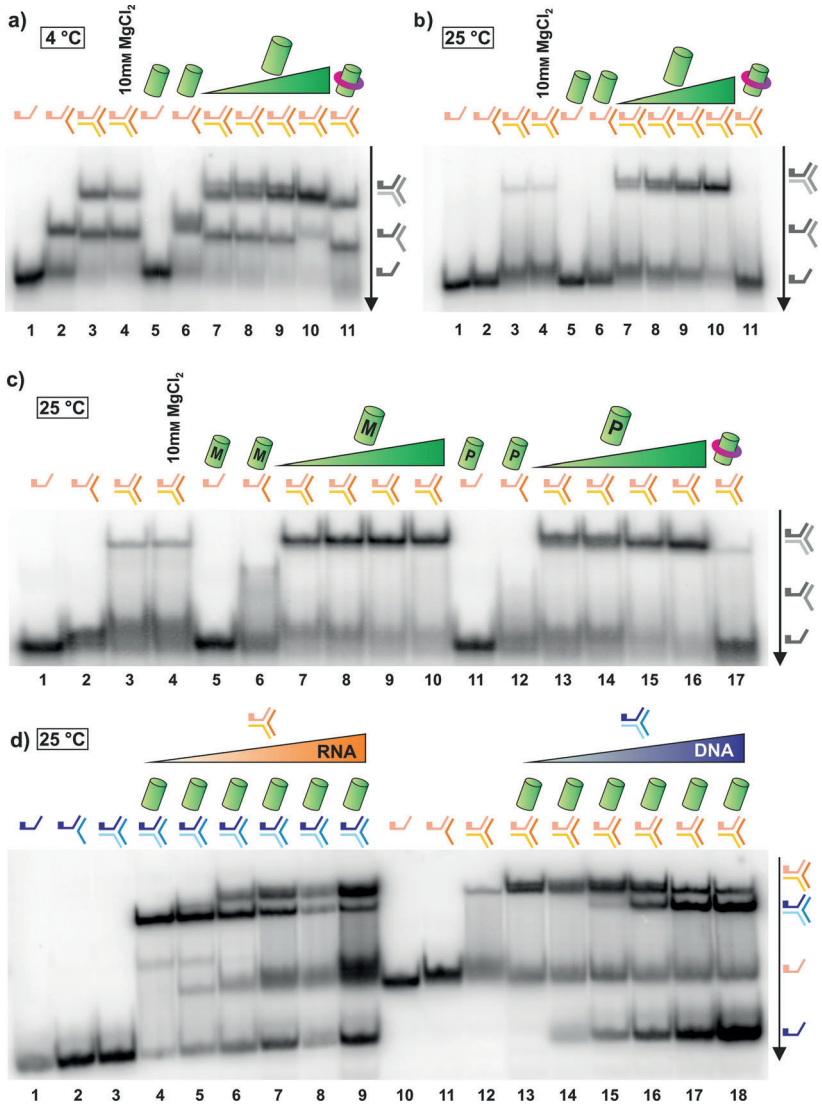

Figure 3. Formation of an RNA 3WJ in the presence of increasing amounts of the di-iron(II) $[Fe_2L_3]^{4+}$ complex followed by 15% native gel electrophoresis (200 nM each S1*, S2, and S3; 100 mM NaCl; 3WJ/cylinder ratios are 1:0.5, 1:1, 1:2, and 1:10 (lanes 7–10 and 13–17)) at a) 4 °C and b) at 25 °C. c) Comparison of stabilization by the *M* versus *P* enantiomers of the cylinder (25 °C). Lanes 11 (a,b) and 17 (c) are controls containing a bulkier cylinder $[Fe_2(L\text{-}CF_3)_3]^{4+}$. Lanes 1–6 (a,b,c) and lanes 11 and 12 (c) are controls without one or two of the RNA strands or the cylinder, as indicated. d) Competition of RNA versus DNA 3WJ formation in the presence of the di-iron(II) complex $[Fe_2L_3]^{4+}$ followed by 20% native gel electrophoresis (200 nM each S1*, S2, and S3; 25 °C; 100 mM NaCl; ratio of preformed 3WJ (RNA = orange, DNA = blue) to cylinder was 1:1 (lanes 4–9 and 13–18)); equivalents of the added 3WJ are 1:0.2, 1:0.5, 1:1, 1:2, and 1:5 (lanes 5–9 and 14–18)). Lanes 1–3 and 10–12 are controls missing either one or two of the RNA/DNA strands or the cylinder, as indicated.

These findings indicate that the perfect size and shape of the di-iron(II) cylinder plays the major role in stabilization of the RNA 3WJ.

To confirm the binding between the RNA and the cylinder we performed UV/Vis and circular dichroism (CD) experiments (Figure S4). Increasing amounts of a racemic mixture of the cylinder, which itself shows no CD signal, were added to the three RNA strands using a constant concentration of RNA and increasing amounts of cylinder. The overlay of the CD spectra of the RNA 3WJ in the presence of up to ten equivalents of racemic cylinder shows that the spectrum of the RNA retains its typical shape (CD signal below 300 nm) throughout the titration, confirming that the A-form conformation of the double helical RNA arms remains unchanged (Figure S4A; note that the concentration of RNA is 50 times higher in the CD experiment than the gel studies). The corresponding UV/Vis spectra show that the presence of the RNA has no effect on the metal-to-ligand charge transfer (MLCT) band between 400 and 650 nm, confirming the structural integrity of the cylinder (Figure S4B). However, in the same MLCT region, the CD spectra show an increased negative elipticity corroborating a binding event between the di-iron(II) cylinder and the RNA.

Having shown that the cylinder stabilizes an RNA 3WJ, the question arises whether the cylinder preferentially binds to DNA or RNA. We established an assay to follow the competition between analogous RNA and DNA 3WJs. Up to five equivalents of RNA 3WJ were added to a constant concentration of the competing DNA 3WJ-cylinder complex. A decrease in DNA 3WJ accompanied by a simultaneous increase in RNA 3WJ was observed (Figure 3D; note, RNA migrates slower on the native gel than DNA). The inverse experiment was conducted and showed the same overall effect: an increase in DNA 3WJ was paralleled by a decrease of RNA 3WJ, although the concurrent increase in single-stranded RNA S1 seemed less pronounced. The difference in the inherent stabilities of the RNA and DNA 3WJs complicates quantification of the cylinder binding preferences; while the RNA 3WJ might be slightly preferred over the DNA 3WJ, it is also more stable in the absence of cylinder, which might be reflected in the experiment. However, despite the inherent structural differences in the binding of the cylinder to the two nucleic acid junctions, they compete with one another for cylinder binding. It appears that the difference in Gibbs free energy for binding must be small and that the interaction between the cylinder and the nucleic acid junctions is sufficiently dynamic to allow for equilibration.

Small-molecule recognition by nucleic acids and the accompanying stabilization of a specific structure or a subsequent structural change are key to natural processes, for example, in riboswitches as well as for medical applications, but are so far only poorly understood. This study is the first of

its kind to characterize in detail the binding of a designed anticancer di-iron(II) supramolecular cylinder to an RNA 3WJ 1) at atomic resolution in the solid state, 2) in solution, and 3) to establish the competition with a respective DNA 3WJ. Both nucleic acid 3WJs were similarly stabilized by the cylinder. This is surprising because of their inherent structural differences and the dynamic nature of the recognition of 3WJs by metal-based drugs.

Experimental Section

The interaction between the cylinder and RNA was investigated by native polyacrylamide gel electrophoresis (PAGE) in which one strand (S1*) was radioactively labeled using [γ-32P]-ATP. CD and UV/Vis titrations were performed at a constant concentration of RNA 3WJ (10 μM) and varying amounts of each di-iron(II) cylinder enantiomer (0.5–10 equiv). Crystals of the cylinder-RNA complex were grown at 20 °C under the following conditions: Tris-HCl (50 mM, pH 8.5), $Mg(OAc)_2$ (165 mM), PEG 400 (15 %). Diffraction data were recorded at the X06DA beamline of the Swiss Light Source (Paul Scherrer Institute, Villigen, Switzerland). Full materials and methods are available online in the Supporting Information.

The atomic coordinates have been deposited with the PDB under accession code 4JIY.

Received: June 13, 2013
Published online: August 23, 2013

Keywords: antitumor agents · bioinorganic chemistry · helicates · RNA recognition · three-way junctions

[1] D. R. Boer, A. Canals, M. Coll, *Dalton Trans.* **2009**, 399 – 414.
[2] a) J. Reedijk, *Chem. Commun.* **1996**, 801 – 806; b) Z. J. Guo, P. J. Sadler, *Adv. Inorg. Chem.* **2000**, *49*, 183 – 306; c) M. J. Hannon, *Pure Appl. Chem.* **2007**, *79*, 2243 – 2261.
[3] K. B. Garbutcheon-Singh, M. P. Grant, B. W. Harper, A. M. Krause-Heuer, M. Manohar, N. Orkey, J. R. Aldrich-Wright, *Curr. Top. Med. Chem.* **2011**, *11*, 521 – 542.
[4] S. Komeda, T. Moulaei, M. Chikuma, A. Odani, R. Kipping, N. P. Farrell, L. D. Williams, *Nucleic Acids Res.* **2011**, *39*, 325 – 336.
[5] B. M. Zeglis, V. C. Pierre, J. T. Kaiser, J. K. Barton, *Biochemistry* **2009**, *48*, 4247 – 4253.
[6] S. N. Georgiades, N. H. Abd Karim, K. Suntharalingam, R. Vilar, *Angew. Chem.* **2010**, *122*, 4114 – 4128; *Angew. Chem. Int. Ed.* **2010**, *49*, 4020 – 4034.
[7] a) A. Oleksi, A. G. Blanco, R. Boer, I. Uson, J. Aymami, A. Rodger, M. J. Hannon, M. Coll, *Angew. Chem.* **2006**, *118*, 1249 – 1253; *Angew. Chem. Int. Ed.* **2006**, *45*, 1227 – 1231; b) L. Cerasino, M. J. Hannon, E. Sletten, *Inorg. Chem.* **2007**, *46*, 6245 – 6251; c) J. Malina, M. J. Hannon, V. Brabec, *Chem. Eur. J.* **2007**, *13*, 3871 – 3877; d) L. A. Howell, M. Searcey, *ChemBioChem* **2009**, *10*, 2139 – 2143.
[8] a) P. B. Glover, P. R. Ashton, L. J. Childs, A. Rodger, M. Kercher, R. M. Williams, L. De Cola, Z. Pikramenou, *J. Am. Chem. Soc.* **2003**, *125*, 9918 – 9919; b) C. A. Puckett, J. K. Barton, *J. Am. Chem. Soc.* **2007**, *129*, 46 – 47; c) U. Schatzschneider, J. Niesel, I. Ott, R. Gust, H. Alborzinia, S. Wolfl, *ChemMedChem* **2008**, *3*, 1104 – 1109; d) O. Zava, S. M. Zakeeruddin, C. Danelon, H. Vogel, M. Gratzel, P. J. Dyson, *ChemBioChem* **2009**, *10*, 1796 – 1800; e) M. Matson, F. R. Svensson, B. Norden, P. Lincoln, *J. Phys. Chem. B* **2011**, *115*, 1706 – 1711.
[9] J. Brunner, J. K. Barton, *J. Am. Chem. Soc.* **2006**, *128*, 6772 – 6773.
[10] a) D. R. Boer, J. M. C. A. Kerckhoffs, Y. Parajo, M. Pascu, I. Uson, P. Lincoln, M. J. Hannon, M. Coll, *Angew. Chem.* **2010**, *122*, 2386 – 2389; *Angew. Chem. Int. Ed.* **2010**, *49*, 2336 – 2339; b) N. Megger, L. Welte, F. Zamora, J. Müller, *Dalton Trans.* **2011**, *40*, 1802 – 1807.
[11] a) C. S. Chow, J. K. Barton, *J. Am. Chem. Soc.* **1990**, *112*, 2839 – 2841; b) N. W. Luedtke, J. S. Hwang, E. C. Glazer, D. Gut, M. Kol, Y. Tor, *ChemBioChem* **2002**, *3*, 766 – 771; c) C. B. Spillane, J. A. Smith, D. P. Buck, J. G. Collins, F. R. Keene, *Dalton Trans.* **2007**, 5290 – 5296; d) A. A. Hostetter, E. G. Chapman, V. J. DeRose, *J. Am. Chem. Soc.* **2009**, *131*, 9250 – 9257; e) H. K. Hedman, F. Kirpekar, S. K. C. Elmroth, *J. Am. Chem. Soc.* **2011**, *133*, 11977 – 11984.
[12] A. Serganov, S. Keiper, L. Malinina, V. Tereshko, E. Skripkin, C. Hobartner, A. Polonskaia, A. T. Phan, R. Wombacher, R. Micura, Z. Dauter, A. Jaschke, D. J. Patel, *Nat. Struct. Mol. Biol.* **2005**, *12*, 218 – 224.
[13] R. T. Batey, S. D. Gilbert, R. K. Montange, *Nature* **2004**, *432*, 411 – 415.
[14] J. Schnabl, P. Suter, R. K. O. Sigel, *Nucleic Acids Res.* **2012**, *40*, D434 – D438.
[15] a) R. Koradi, M. Billeter, K. Wuthrich, *J. Mol. Graphics* **1996**, *14*, 51 – 55, 29 – 32; b) Accelrys Software Inc., Discovery Studio Modeling Environment, Release 3.5, San Diego **2012**.